The Spine Journal 23 (2023) 599–608

Basic Science

Three-dimensional correction of scoliosis by a double spring reduction system as a dynamic internal brace: a pre-clinical study in Göttingen minipigs

Justin V.C. Lemans, MD[a,*], Sebastiaan P.J. Wijdicks, MD, PhD[a], Gerrit Overweg, MS[b], Edsko E.G. Hekman, MS[b], Tom. P.C. Schlösser, MD, PhD[a], René M. Castelein, MD, PhD[a], Gijsbertus J. Verkerke, PhD[b,c], Moyo C. Kruyt, MD, PhD[a,d]

[a] *University Medical Center Utrecht, Department of Orthopaedic Surgery, PO Box 85500, 3553 GA, Utrecht, The Netherlands*
[b] *University of Twente, Department of Biomechanical Engineering, PO Box 217, 7500 AE, Enschede, The Netherlands*
[c] *University of Groningen, University Medical Center Groningen, Department of Rehabilitation Medicine, PO Box 30.001, 9700 RB, Groningen, The Netherlands*
[d] *University of Twente, Department of Developmental BioEngineering, PO Box 217, 7500 AE, Enschede, The Netherlands*
Received 13 July 2022; revised 7 October 2022; accepted 26 October 2022

Abstract

BACKGROUND CONTEXT: Adolescent idiopathic scoliosis (AIS) is a major skeletal deformity that is characterized by a combination of apical rotation, lateral bending and apical lordosis. To provide full 3D correction, all these deformations should be addressed. We developed the Double Spring Reduction (DSR) system, a (growth-friendly) concept that continuously corrects the deformity through two different elements: A posterior convex Torsional Spring Implant (TSI) that provides a derotational torque at the apex, and a concave Spring Distraction System (SDS), which provides posterior, concave distraction to restore thoracic kyphosis.

PURPOSE: To determine whether the DSR components are able to correct an induced idiopathic-like scoliosis and to compare correction realized by the TSI alone to correction enforced by the complete DSR implant.

STUDY DESIGN/SETTING: Preclinical randomized animal cohort study.

PATIENT SAMPLE: Twelve growing Göttingen minipigs.

OUTCOME MEASURES: Coronal Cobb angle, T10-L3 lordosis/kyphosis, apical axial rotation, relative anterior lengthening.

METHODS: All mini-pigs received the TSI with a contralateral tether to induce an idiopathic-like scoliosis with apical rotation (mean Cobb: 20.4˚; mean axial apical rotation: 13.1˚, mean lordosis: 4.9˚). After induction, the animals were divided into two groups: One group (N=6) was corrected by TSI only (TSI only-group), another group (N=6) was corrected by a combination of TSI and SDS (DSR-group). 3D spinal morphology on CT was compared between groups over time. After 2 months of correction, animals were euthanized.

RESULTS: Both intervention groups showed excellent apical derotation (TSI only-group: 15.0˚ to 5.4˚; DSR-group: 11.2˚ to 3.5˚). The TSI only-group showed coronal Cobb improvement from 22.5˚ to 6.0˚, while the DSR-group overcorrected the 18.3˚ Cobb to -9.2˚. Lordosis was converted to kyphosis in both groups (TSI only-group: -4.6˚ to 4.3˚; DSR-group: -5.2˚ to 25.0˚) which was significantly larger in the DSR-group ($p<.001$).

CONCLUSIONS: The TSI alone realized strong apical derotation and moderate correction in the coronal and sagittal plane. The addition of distraction on the posterior concavity resulted in more coronal correction and reversal of induced lordosis into physiological kyphosis.

FDA device/drug status: DSR Implant - Not approved for this indication.

Author disclosures: ***JVCL:*** Grant: Stryker (F). ***SPJW:*** Grant: Stryker (F). ***GO:*** Nothing to Disclose. ***EEGH:*** Grant: Stryker (F). ***TPCS:*** Grant: Stryker (F). ***RMC:*** Grant: Stryker (F). ***GJV:*** Grant: Stryker (F). ***MCK:*** Grants: Stryker (F), Miscellaneous (F).

*Corresponding author. University Medical Center Utrecht, Department of Orthopaedic Surgery, PO Box 85500, 3553 GA, Utrecht, The Netherlands.

E-mail address: j.v.c.lemans-3@umcutrecht.nl (J.V.C. Lemans).

https://doi.org/10.1016/j.spinee.2022.10.012

CLINICAL SIGNIFICANCE: This study shows that dynamic spring forces could be a viable method to guide the spine towards healthy alignment, without fusing it or inhibiting its growth.

Keywords: Double Spring Reduction; Growth; Growth-friendly; Minipigs; Non-fusion; Scoliosis; Spine

Introduction

Adolescent idiopathic scoliosis (AIS) is a major skeletal deformity with pulmonary and cardiac consequences [1,2], that is characterized by a combination of apical rotation, lateral bending and apical lordosis. These deformities are largely due to anterior lengthening that is mainly located in the intervertebral disc (IVD) [3–6]. To achieve correction in all planes, all these deformations should be addressed, with specific attention to sufficient posterior concave distraction to accommodate the longer anterior column, so that it may rotate back into the midline.

Current treatments for adolescent idiopathic scoliosis (AIS) either stabilize the curve with bracing or surgically fuse the spine. Bracing can be effective in preventing curve progression, but only with strict patient compliance to wear the brace >16 hours per day [7,8]. Even then, residual curves can be considerable [7]. Spinal fusion is more effective in correcting the 3D morphology of the spine, however at the cost of spinal mobility, which adversely affects long-term quality of life of these patients [9].

Only at very young age, serial (Mehta) casting is known to be able to "cure" the spine; that is to resolve the deformity while retaining a flexible spine [10]. However, such permanent rigid casts, which apply large corrective forces, are not tolerated by older children.

To achieve similar results for these patients, an internal brace could possibly overcome many of the disadvantages of serial casts. Most importantly, strategic forces can be exerted on the spine with 100% compliance. By using dynamic and flexible implants, such application of prespecified forces and torques is possible. For this purpose, we developed the Double Spring Reduction (DSR) implant (Fig. 1), which consists of two different spring implants, the torsional spring implant (TSI) and the spring distraction system (SDS). Together, these temporary flexible implants provide continuous apical axial torque (TSI) and posterior distraction forces (SDS) to the spine during the years that it has a chance to mature into a reduced and stable configuration. The implant can accommodate growth, and can therefore be used when the child has not yet reached skeletal maturity. This "growth-friendly" feature not only allows for early correction of AIS curves of older children, it also allows for treatment of "tweeners" aged 9–11, where current "growth-friendly" implant results are often disappointing when compared to results of spinal fusion.

Previous studies have investigated the concept of the TSI, concluding that it has the potential to provide strong apical (de-)rotation with only a very small increase in spinal stiffness [11,12]. A recent preclinical study by our group in growing Göttingen minipigs has shown that the TSI, combined with a flexible tether, was able to induce a morphologically idiopathic-like scoliosis whilst retaining mobility and growth [13]. After implant removal, the deformity remained and was shown to reside mainly in the IVD, indicating permanent spinal changes similar to those seen in human AIS.

We performed the current study to determine whether the internal brace concept (DSR) is able to correct the established idiopathic-like scoliosis. In addition, we investigated whether correction with torsion alone is equally effective when compared to a combination of both torsion and posterior distraction.

Materials and methods

Ethical approval

This study was performed in the AAALAC certified experimental surgery animal laboratory of Utrecht University. Ethical approval was granted by the Animal Experiment Committee of Utrecht University before the start of this study (AVD 115002016804).

Study design

The current study consisted of 2 phases (Fig. 2). Phase 1 was the induction phase, wherein a scoliosis was induced in 12 growing Göttingen minipigs through implantation of a left-sided unilateral, posterior tether combined with a contralateral TSI, tensioned to provide 2 Nm of axial torque [13]. After 3 months of induction, the curves were confirmed with CT scans and phase 2, the reduction phase, was initiated. All 12 minipigs were operated again, the induction forces were released and animals were randomized into two groups, each undergoing a different method of scoliosis reduction: (1) Reduction by only de-rotating the curve apex with the torsional TSI (TSI only-group, N=6), or (2) Reduction by combining the TSI with the concave distraction implant SDS (DSR-group, N=6). After the reduction surgery, 2 months of follow-up was allowed for spinal remodeling. Then, the animals were euthanized. Spinal morphology between groups was compared with 3D imaging at several timepoints.

Animal model

The Ellegaard Göttingen minipig is bred specifically for research purposes, and has a predictable linear growth curve

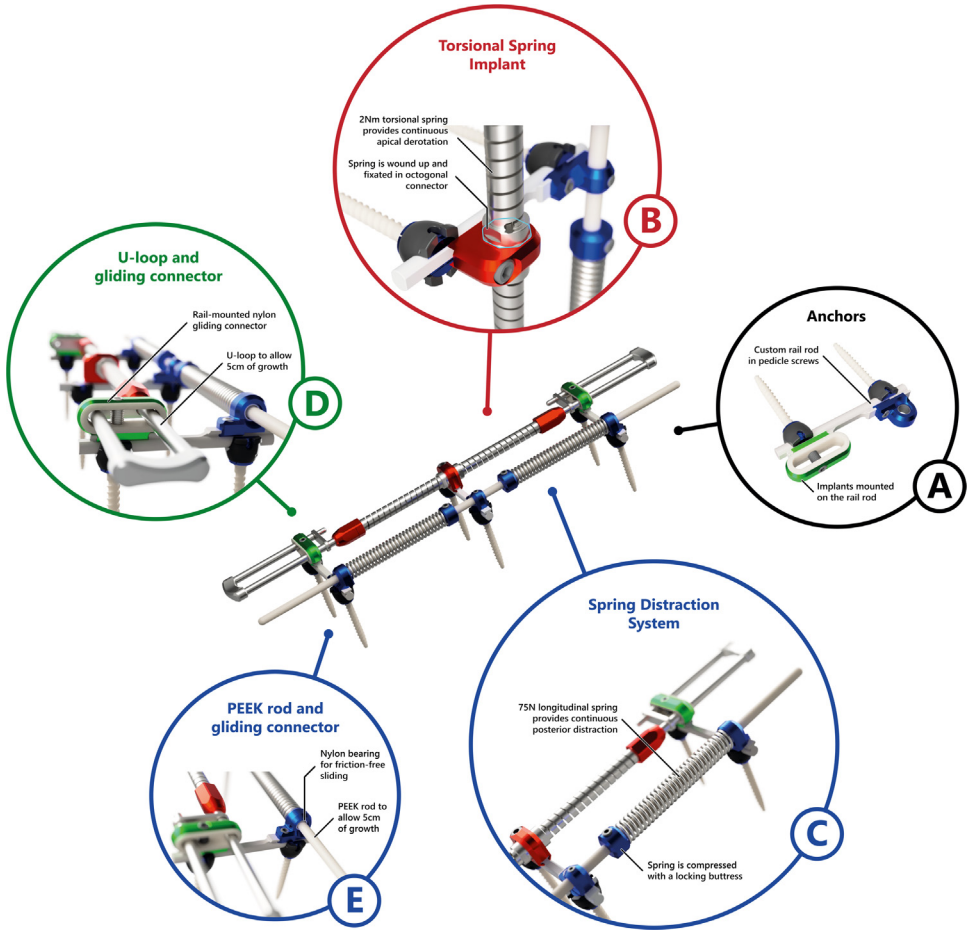

Fig. 1. Double Spring Reduction implant. The Double Spring Reduction implant consists of two different springs that are mounted on top of custom rail rods (A). The torsional spring implant (TSI) is fixated to the curve convexity (B) and exerts a continuous axial torque to the apical level. The spring distraction system (C) is fixated to the curve concavity. Both the torsional spring implant (D) and spring distraction system (E) have sliding connectors that allow for spinal growth.

from birth to 2 years of age, which can be translated very well to pediatric spinal growth [14,15]. In addition, spinal anatomy is similar in size and shape to human pediatric anatomy. The animals can be housed in groups, and their small stature makes animal husbandry less cumbersome as compared to larger cattle. Whilst the minipig spine is positioned horizontally and not upright like the human spine, it serves as a representative scoliosis model, since it has been shown that muscle forces in quadrupeds ensure similar axial compressive force vectors comparable to vertical human spinal loading [16].

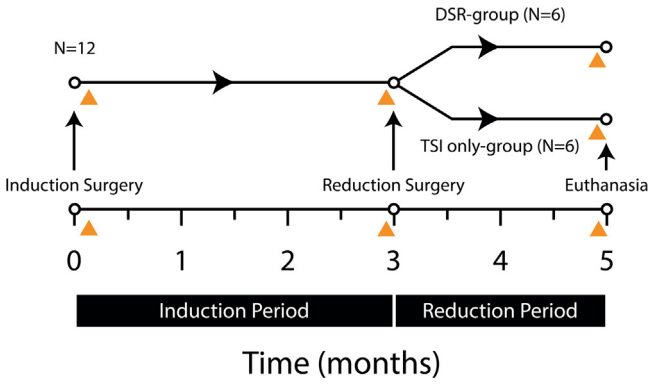

Fig. 2. Experiment timeline. In 12 animals, scoliosis induction is performed with a left-sided tether and 2 Nm of apical torque to the right. After 3 months, animals are divided into two groups for a reduction period of 2 months: Six animals received only the TSI-implant, while six were treated with the complete DSR-implant (ie, derotation and distraction). The orange triangles denote moments where spinal morphology was analyzed with imaging.

Double spring reduction implant

The complete internal brace, the DSR implant (Fig. 1), consists of two different flexible components: (1) the TSI, and (2) the SDS. These are positioned on either side of the posterior spine and mounted on posterior pedicle screw anchors. Both components deliver continuous forces and torques in all planes, while allowing mobility and growth of the spine.

The TSI (Fig. 1B) consists of two in-line nickel-cobalt alloy (MP35N) torsion springs with titanium U-loops at the upper- and lower ends that can slide through the upper and lower anchor bearings that are mounted to T10 cranially

and L3 caudally. At the apex (T14), the connector between both springs can be pre-tensioned with 2 Nm by 45° of rotation and then be mounted to the apical anchor to deliver the axial torque. The U-shaped loops (Fig. 1D) are designed so that with spinal growth, the combined torsional stiffness of the springs and the loops increase, causing the corrective torque to remain essentially the same in spite of the decreasing pre-tension angle. This counteracts the decrease in torque that would otherwise take place due to apical derotation over time. The TSI has a growth potential of 100 mm, 50 mm on both the cranial- and caudal side and adds <20% additional spinal stiffness, which is far less than what is found with contemporary correction implants [11].

The SDS (Fig. 1C) consists of two titanium (ASTM Grade 19) coil springs around a flexible 4mm polyether ether ketone (PEEK) rod. The rod slides through nylon bearings (Fig. 1E) on the upper and lower anchor, and has a growth potential of 50mm on each side. The central part is mounted to the apical anchor to prevent buckling. The springs are tensioned to deliver 75 N with a simple buttress that is fixated to the rod. Distraction force linearly decreases with length gain based on the spring constant (k) and Hooke's law ($F_d = k \cdot x$). The SDS principle has been used in our clinic for treatment of early-onset scoliosis patients, with satisfactory curve correction and remaining spinal growth [17–19].

Surgical technique

The surgical induction technique has been described previously, it is summarized here for completeness (Fig. 3) [13]. After standard surgical preparation of the minipigs, exposure through a dorsal midline approach was performed spanning levels T10, T14 (Göttingen minipigs have 15 thoracic vertebrae) and L3. At these three levels, bilateral pedicle screws were implanted under fluoroscopic guidance (Mesa Small Stature, Stryker, Kalamazoo, MI, USA). Custom rail rods were then mounted to connect the left and right pedicle screws (Fig. 1A) and create a cranial, apical, and caudal anchor. Between each anchor, three vertebral bodies, four IVDs and four pairs of apophyseal joints were left untouched.

For scoliosis induction, an UHMWPE tether (Dyneema, DSM, Geleen, The Netherlands) was looped around the cranial and caudal anchors on the left side and closed tight but without tension. The TSI was mounted on the right side, with bearings that fit on the rails cranially and caudally, leaving the apical connector unlocked. The apical part of the torsional spring (Fig. 1B) was then rotated 45° in the axial plane with a custom wrench (to induce a right-sided scoliosis) and was subsequently locked to the apical rail (Fig. 3A/B). Immediately following surgery, radiographic,- and CT imaging was obtained. The animals were returned to their housing units where they were kept in groups and fed ad libitum.

Three months following the induction surgery, the animals were anaesthetized and CT scans were made to visualize scoliosis morphology and signs of implant failure. After exposure, the integrity of the tether was checked before it was released and subsequently removed. On the right side, the apical connector of the TSI was unlocked and returned back to neutral. Mobility of the spine was assessed manually under dynamic fluoroscopic imaging. The TSI was then rotated 45° in the other direction, to reduce the rotational deformity and was then locked again. After randomization, the wound was then either closed immediately (TSI only-group) or an SDS was first implanted on the concave side (DSR-group). The SDS rod was fixated to the apical anchor and could slide through two sliding bearings that were mounted on the cranial and caudal anchor. Then the springs were tensioned to 70±5 N with the buttress.

After 2 months of follow-up, CT and radiography were performed. Following this, the minipigs were euthanized by intracardiac injection of pentobarbital, compliant with the 2020 American Veterinary Medical Association guidelines for the euthanasia of animals [20]. The implants were removed and checked for damage and the spines were manually tested for flexibility.

Radiographic analysis

Coronal Cobb angle and instrumented kyphosis were measured on the coronal and sagittal CT reconstructions, More detailed analysis of axial rotation and relative anterior-posterior and convex-concave lengthening of both the intervertebral discs and vertebral bodies was performed using the ScoliosisAnalysis 4.1 software (Imaging Sciences Institute, Utrecht University). This validated method has been used previously and is detailed in Fig. 4 [3–5]. First, the superior- and inferior vertebral endplates and spinal canals were segmented in the true transverse plane (ie, accounting for coronal and sagittal tilt). Then, the centroid (ie area center) of the vertebral endplate and spinal canal was calculated and the anterior-posterior (AP) axis, which intersects both centroids, was drawn. The two points where the AP axis intersects the segmented endplate were defined to be the anterior and posterior midline points of the endplate. A line perpendicular to the AP axis, intersecting the centroid of the endplate, defined the left-right axis, and the left and right borders of the vertebra. The x- y- and z-coordinates of each point were determined and the anterior, posterior, concave, and convex lengths of each vertebra and intervertebral disc could then be calculated geometrically using the formula:

$$d(P1,\ P2) = \sqrt{(x1 - x2)^2 + (y1 - y2)^2 + (z1 - z2)^2}$$

Where $P1$ and $P2$ are two similar points on two different endplates (eg, anterior, posterior, left, right) that are to be compared, d is the shortest distance between these points, and $x1, 2$, $y1,2$ and $z1, 2$ are the respective 3D coordinates. By comparing the upper- and lower endplate of the same vertebra, lengths corresponding to that vertebra can be calculated, while comparing the lower endplate of one vertebra

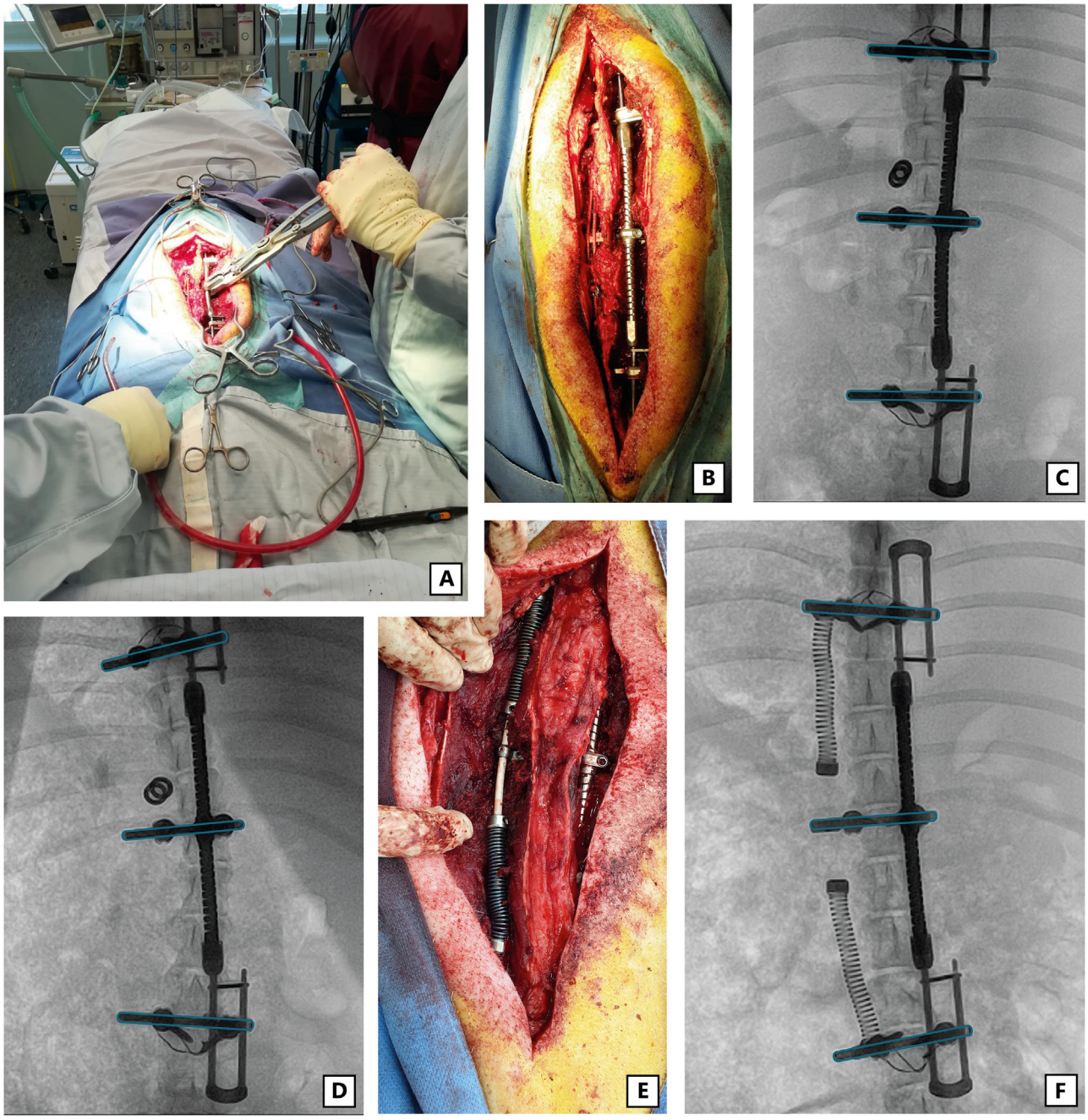

Fig. 3. Induction- and reduction surgery. (A) During induction, the TSI is wound up by rotating it 45° in the clockwise direction (looking in the caudo-cranial direction), to deliver 2Nm torque. (B) Close-up of the TSI (right) and the implanted tether (left). (C) Radiograph immediately following induction surgery. The rails are outlined in blue to highlight the change in coronal deformity over time. The buckles with which the tethers are fixated can be seen on the left, the tether itself is radiolucent. (D) After 3 months, the scoliosis can be seen, including axial rotation. Also note the spinal growth seen as translation of the U-loops relative to the cranial and caudal anchors. (E) During the reduction surgery, the torsional spring force is reversed and two distraction springs on a (radiolucent) flexible PEEK rod are fixated to the left-side. (F) After 2 months, the scoliosis was reduced in the axial and sagittal plane, and was even overcorrected in the coronal plane.

with the upper endplate of the vertebra below yields values corresponding to the IVD space. Axial rotation of an endplate was defined as the angular difference between its AP axis relative to the AP axis of L3. The axial rotation of a vertebral body was determined by averaging the AP axis of the upper- and lower endplate. This yields a difference in rotation between the apical level (T14) and the most cranial (T10) and most caudal (L3) instrumented level. The apical rotation was then obtained by taking the mean of both rotation differences.

Statistical analysis

Prospectively, a power calculation was performed based on our earlier induction animal study [13]. The study was

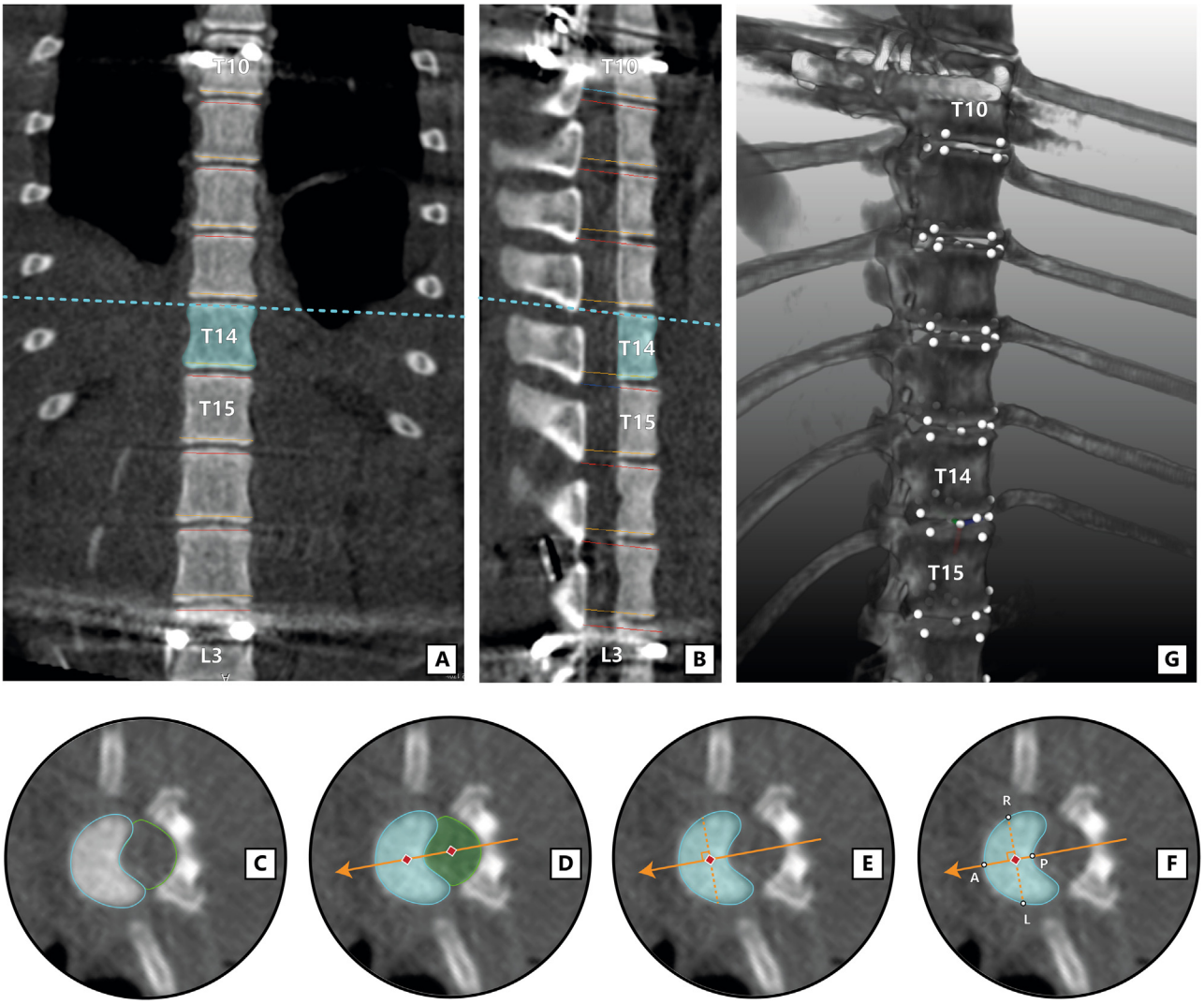

Fig. 4. Radiographic measurements. The endplates of each investigated vertebra (T14 in example above) are segmented. (A–B) First, lines are drawn that correct for coronal (A) and sagittal (B) tilt of each endplate, so that the corresponding axial view corresponds to the true axial plane [3]. (C) In this plane, the endplate (blue) and spinal canal (green) are manually segmented. (D) The ScoliosisAnalysis v4.1 software computes the centroid of both the vertebral body and the spinal canal (red diamonds). The line through these centers defines the vertebral anterior-posterior axis (orange arrow). (E) A line perpendicular to this axis, intersecting the centroid of the vertebral body is then constructed (dashed orange line). (F) Where these two lines intersect the segmentation of the vertebral body, the following points are drawn: anterior (A), posterior (P), left (L) and right (R). (G) The x-, y- and z-coordinates of each point of each endplate are extracted, and relevant lengths and angles between endplates are calculated.

powered to show a difference in correction capabilities between the DSR-group and the TSI only-group after the introduction of the reduction implants. To detect a difference in coronal Cobb angle between groups of 5° (SD 3.0), with a power of 80% and an alpha of 0.05, six animals per group were needed.

Differences in curve morphology between start of the induction period (immediately following induction surgery) and the end of the induction period (after 3 months, just before reduction surgery) were calculated for all 12 animals and shown as mean ± SD. Following this, paired t-tests comparing both timepoints were performed. If the residuals of differences were non-parametric, the Wilcoxon-signed rank test was performed. For the analysis of the reduction period, 2 way repeated measurement ANOVA was performed comparing both the DSR- and TSI-groups over time. Two-tailed significance for all analyses was set at p=.05. Statistical analyses and data visualization were performed with GraphPad Prism 9.2.0. (Graphpad Software, San Diego, CA, USA).

Results

General outcomes and complications

Mean age of the animals during the induction surgery was 7.4 months and mean weight was 20.3 kg, with no significant difference between groups. Weight increased in

5 months to 34.3 kg according to their normal growth charts [14]. During both the induction- and reduction phase, there were no major complications or malpositions of pedicle screws. All tethers functioned as expected and were intact and removed during the reduction surgery. The spines remained flexible in the instrumented segment and the axial torque was successfully inverted in all minipigs. One of the minipigs suffered a deep surgical site infection following reduction surgery. Subfascial pus collections were seen on the CT scan obtained pre-euthanasia, although no clinical symptoms of infection were observed in the months before. Tissue and pus cultures obtained post-euthanasia showed infection with Trueperella pyogenes. All TSI implants were intact upon removal with no signs of substantial wear of the bearings. In one animal in the DSR-group, the SDS PEEK sliding rod buckled out which negatively influenced the distraction force. Curve morphology results of this minipig were included in all analyses.

Radiographic outcomes

Significant changes were induced in all evaluated radiological parameters during the induction period (Table 1). Cobb angle increased from 6.2˚ immediately postoperatively, to 20.4˚ after 3 months. Instrumented kyphosis changed from 6.2˚ to -4.9˚. Axial rotation of the apical level increased from 6.5˚ to 13.1˚ at the end of induction. The anterior spine lengthened during induction, with modest but significant changes in the vertebral bodies (A−P ratio from 0.98 − 0.99), and larger changes in the IVD (A-P ratio from 1.12−1.19).

Changes after the 2 month reduction period for both groups are shown in Table 2. For the TSI only-group, Cobb angle reduced from 22.5˚ to 6.0˚. For the DSR-group, the curve was overcorrected from 18.3˚ to -9.2˚. The change in coronal curve was significantly larger in the DSR-group. For the sagittal plane, the instrumented kyphosis in the TSI only-group changed from -4.6˚ (ie, lordosis) at the end of induction to 4.3˚ (ie, kyphosis) at the end of reduction. In the DSR-group, a change from lordosis to kyphosis was seen as well, from -5.2˚ to 25.0˚. The induced kyphosis was significantly greater in the DSR-group. In the axial plane, the mean apical axial rotation (ie, the relative rotation of level T14 compared to the mean rotation of the most cranial and caudal instrumented level) for the TSI only-group decreased from 15.0˚ to 5.4˚. For the DSR-group, this rotation similarly decreased from 11.2˚ to 3.5˚. Fig. 5 shows the mean rotation per level for each of the groups. In both groups, axial rotation can be observed immediately following induction surgery. In terms of distribution of rotation at the end of induction, a gradual increase is observed from the non-apical areas towards the apical area. In both groups, the rotation appears to be symmetrically distributed between the cranial and caudal part of the spine.

Both the TSI only-group and DSR-group were able to (partly) reduce the anterior lengthening of the IVD during the reduction period (Fig. 6). However, only in the DSR treatment, did we also find a significant posterior lengthening of the vertebral body, indicating asymmetrical growth (A−P ratio 0.99−0.97).

Discussion

The current study investigated the potential of reducing scoliosis with instrumented apical derotation alone (TSI only-group) or in combination with posterior distraction (DSR-group). We used the same TSI implant to first induce scoliosis, a method that we previously showed to generate a very predictable idiopathic-like spinal deformity that remained for months, even after removal of the implants [13].

By applying torque only (with the TSI), almost complete reduction of axial rotation could be achieved within 2 months. This resulted in correction of the coronal and sagittal plane as well, likely as a consequence of coupled motions in the spine [21,22], but complete reduction could not be achieved. By adding a distraction force (SDS) to the TSI (thus utilizing the DSR concept), considerably more correction and even over-correction was obtained. This correction could be related directly to reduction in the typical relative anterior lengthening that is mainly present in the IVD, a phenomenon that we described extensively for

Table 1
3D curve morphology during induction period

	Immediately after induction surgery (N=12)	End of induction period (N=12)	*p* value
Coronal Cobb angle (˚)	6.2±3.2	20.4±4.3	<0.001
Instrumented kyphosis (˚)*	6.2±5.4	-4.9±5.3	<0.001
Apical axial rotation (˚)	6.5±2.9	13.1±5.6	<0.001
Relative anterior lengthening†			
Total A-P ratio	1.01±0.01	1.02±0.01	<0.001
Vertebral body A-P ratio	0.98±0.01	0.99±0.01	0.049
Intervertebral disc A-P ratio	1.12±0.08	1.19±0.04	<0.001

* Negative value represents a lordosis in the instrumented segment.
† A-P ratio >1 denotes longer anterior length compared to posterior length.

Table 2
3D curve morphology during reduction period

	TSI only-group (N=6)			DSR-group (N=6)			p value between groups§
	End of induction period	End of reduction period	p value (TSI only-group)‡	End of induction period	End of reduction period	p value (DSR-group)‡	
Coronal Cobb angle (°)	22.5±3.9	6.0±2.3	<0.0001	18.3±3.1	-9.2±7.3	<0.0001	0.0123
Instrumented kyphosis (°)*	-4.6±4.4	4.3±3.9	0.0015	-5.2±5.6	25.0±6.8	<0.0001	<0.0001
Apical axial rotation (°)	15.0±3.7	5.4±3.4	0.0130	11.2±4.6	3.5±5.1	0.0202	0.6494
Relative anterior lengthening†							
Total A-P ratio	1.02±0.001	1.01±0.01	0.0109	1.03±0.01	0.98±0.01	<0.0001	0.0004
Vertebral body A-P ratio	0.99±0.01	0.98±0.01	0.4055	0.99±0.01	0.97±0.01	<0.0001	0.0017
Intervertebral disc A-P ratio	1.19±0.03	1.12±0.04	0.0239	1.19±0.04	1.05±0.07	0.0004	0.0622

* Negative value represents a lordosis in the instrumented segment.
† A-P ratio >1 denotes longer anterior length compared to posterior length.
‡ p value related to the change over time within one group (paired t-test).
§ p value related to the change over time between groups (2-way repeated measure ANOVA).

human scoliosis [3−5]. This finding shows that by combining axial torque and concave distraction (DSR) we have a powerful tool to correct scoliosis simultaneously in all planes. However, it also indicates that the forces should be tailored to the specific condition as overcorrection is a risk. One way to mitigate this is to selectively release one of the forces when full correction in that plane has been achieved. Due to the position of the implant and the familiarity with this approach, this would be a minimally invasive procedure. Besides full correction, we observed that normal growth and mobility of the instrumented segment was maintained.

In our opinion, this brings us one step closer to our goal of curing scoliotic spines in adolescents. This would require a paradigm shift in scoliosis care, namely that patients be treated surgically at an earlier age, perhaps already in the range of curves which are currently braced (30°−50°). We propose that DSR may replace those brace treatments that are likely to fail or those that will likely end with considerable remaining curves. Compared to bracing, DSR has the obvious drawback of requiring a surgical intervention. However, the implant can be inserted less invasively and after insertion, the burden for both patients and caregivers will be much lower as there are no mobilization restrictions and no compliance issues. Furthermore, the transmission of forces through DSR's internal brace concept is superior to that of an external brace, especially for correction of the axial rotation.

DSR is not the first surgical technique to attempt gradual correction of AIS curves in the growing spine. In recent years, an increasing body of evidence has been generated wherein growth modulation has been achieved through anterior vertebral body tethering (AVBT). However, we believe AVBT has several disadvantages when compared to DSR. It halts growth on the convex side, and is limited in the amount of correction that can be achieved, in particular in the axial plane [23]. In contrast, DSR is able to continuously correct all planes simultaneously, whilst stimulating (not halting) the shorter concavity of the curve.

In addition to its use in AIS patients, DSR could also be used in growing EOS patients, as DSR has considerable advantages over current "growth-friendly" implants. Especially in older EOS patients (ie, "tweeners"), curve correction is often poor and complication rates are high, which has led to several studies concluding that spinal fusion in these patients may be more effective than "growth-friendly" treatment [24,25]. DSR allows for increased apical derotation, while its flexibility decreases stress- shielding of the spine, which may ultimately lead to reduced implant stresses and implant complications [11,26]. However, since the time interval until skeletal maturation is longer than for AIS, DSR treatment of EOS patients may be somewhat unpredictable, an issue that is currently also observed in younger patients (Sanders 1−2) treated with AVBT [23,27].

Limitations of the current study are mainly related to the use of an animal model. Although the scoliosis

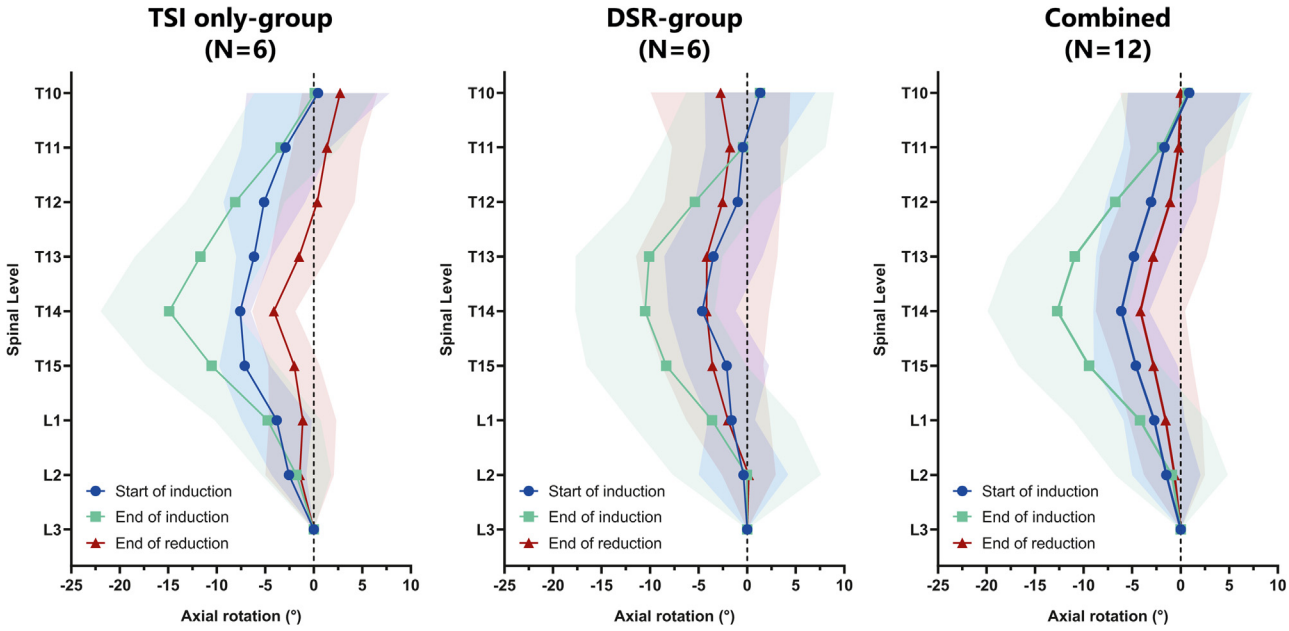

Fig. 5. Vertebral axial rotation over time. Cumulative rotation of each vertebra relative to the most distal instrumented level (L3). Mean values and standard deviations (shaded area) are shown. Negative values represent a right-sided rotation.

morphologically resembles human scoliosis more than any other animal model, we do not know exactly how a human scoliotic spine will react to these dynamic forces. Based on our clinical experience using only spring distraction forces, especially idiopathic curves can be very difficult to correct or even control, suggesting that the etiological mechanism remains to be overcome [18,19]. Future fundamental and clinical studies will teach us more on this important aspect of the technology.

Conclusion

In our representative idiopathic-like, scoliotic animal model, correction with only axial torque was able to correct rotation of the apex, in addition to partially correcting the coronal curve, apical lordosis and anterior lengthening of the IVD. However, adding posterior distraction to the axial torque (DSR), resulted in stronger correction in the coronal and sagittal planes, in addition to posterior vertebral growth modulation.

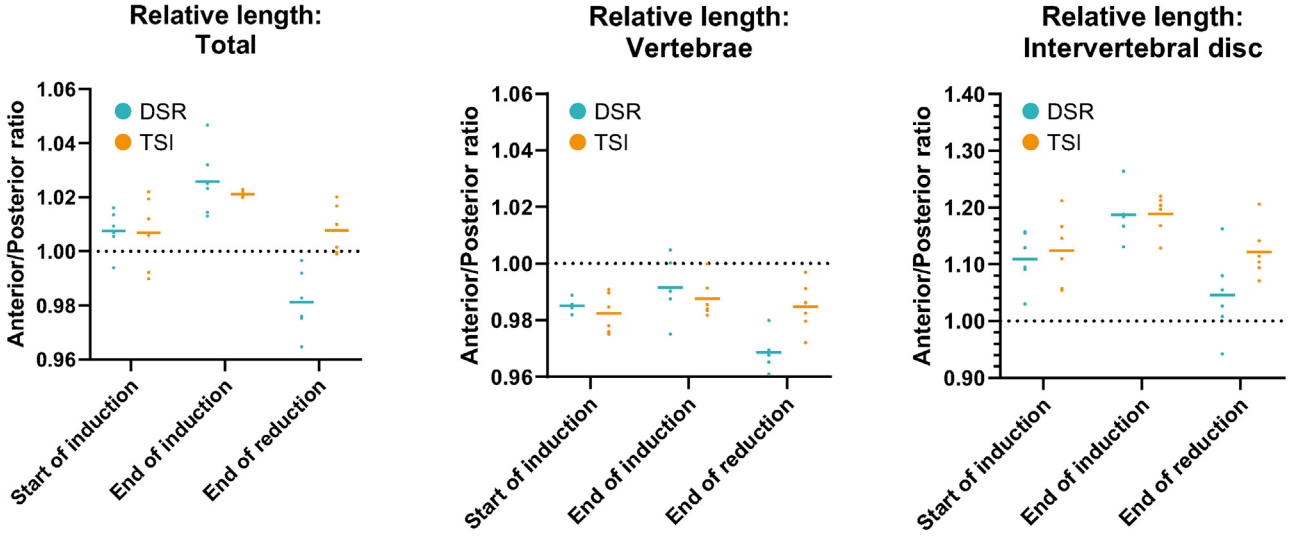

Fig. 6. Relative anterior spinal lengthening over time. The relative lengths (anterior length/posterior length) of both groups are shown, for the total spine (ie, vertebral bodies + intervertebral discs, left), for the vertebral bodies alone (middle) and for the intervertebral discs alone (right). A value > 1 indicates a segment that is longer anteriorly than posteriorly, as is common in human scoliosis.

Acknowledgments

The current study was funded through a K2M (now Stryker Spine) Research Grant (R4198). The funder had no influence on the design of the study, collection, analysis and interpretation of the data, writing of the manuscript, nor on the decision to publish.

René Castelein and Moyo Kruyt are co-inventors of patent US10610262/AU2018202651, which forms the basis for the development of the spring distraction system (SDS). They are also co-founder of CRESCO spine, a spin-off company that aims to valorize SDS. Edsko Hekman and Gijsbertus Verkerke are co-inventors of patent US9687277B2/EP2849663B1, which forms the basis for the development of the torsional spring implant.

Declarations of Competing Interests

One or more of the authors declare financial or professional relationships on ICMJE-TSJ disclosure forms.

References

[1] Sarwahi V, Galina J, Atlas A, Gecelter R, Hasan S, Amaral TD, et al. Scoliosis surgery normalizes cardiac function in adolescent idiopathic scoliosis patients. Spine (Phila Pa 1976) 2021. https://doi.org/10.1097/BRS.0000000000004060.

[2] Farrell J, Garrido E, Vavruch L, Schlösser TPC. Thoracic morphology and bronchial narrowing are related to pulmonary function in adolescent idiopathic scoliosis. J Bone Joint Surg Am 2021. https://doi.org/10.2106/JBJS.20.01714.

[3] Schlösser TPC, van Stralen M, Brink RC, Chu WCW, Lam T-P, Vincken KL, et al. Three-dimensional characterization of torsion and asymmetry of the intervertebral discs versus vertebral bodies in adolescent idiopathic scoliosis. Spine (Phila Pa 1976) 2014;39:E1159–66. https://doi.org/10.1097/BRS.0000000000000467.

[4] Brink RC, Schlösser TPC, Colo D, Vavruch L, van Stralen M, Vincken KL, et al. Anterior spinal overgrowth is the result of the scoliotic mechanism and is located in the disc. Spine (Phila Pa 1976) 2017;42:818–22. https://doi.org/10.1097/BRS.0000000000001919.

[5] de Reuver S, Brink RC, Homans JF, Vavruch L, Tropp H, Kruyt MC, et al. Anterior lengthening in scoliosis occurs only in the disc and is similar in different types of scoliosis. Spine J 2020. https://doi.org/10.1016/j.spinee.2020.03.005.

[6] Castelein RM, Pasha S, Cheng JCY, Dubousset J. Idiopathic scoliosis as a rotatory decompensation of the spine. J Bone Miner Res 2020;35. https://doi.org/10.1002/jbmr.4137.

[7] Weinstein SL, Dolan LA, Wright JG, Dobbs MB. Effects of bracing in adolescents with idiopathic scoliosis. N Engl J Med 2013;369:1512–21. https://doi.org/10.1056/nejmoa1307337.

[8] Katz DE, Herring JA, Browne RH, Kelly DM, Birch JG. Brace wear control of curve progression in adolescent idiopathic scoliosis. J Bone Jt Surgery-American Vol 2010;92:1343–52. https://doi.org/10.2106/JBJS.I.01142.

[9] Helenius I, Remes V, Yrjönen T, Ylikoski M, Schlenzka D, Helenius M, et al. Harrington and cotrel-dubousset instrumentation in adolescent idiopathic scoliosis: long-term functional and radiographic outcomes. J Bone Jt Surg - Ser A 2003;85. https://doi.org/10.2106/00004623-200312000-00006.

[10] Mehta MH. Growth as a corrective force in the early treatment of progressive infantile scoliosis. J Bone Jt Surg - Ser B 2005;87-B:1237–47. https://doi.org/10.1302/0301-620X.87B9.16124.

[11] Wessels M, Hekman EEG, Verkerke GJ. Mechanical behavior of a novel non-fusion scoliosis correction device. J Mech Behav Biomed Mater 2013;27:107–14. https://doi.org/10.1016/j.jmbbm.2013.07.006.

[12] Wessels M, Hekman EEG, Kruyt MC, Castelein RM, Homminga JJ, Verkerke GJ. Spinal shape modulation in a porcine model by a highly flexible and extendable non-fusion implant system. Eur Spine J 2016;25:2975–83. https://doi.org/10.1007/s00586-016-4570-9.

[13] Wijdicks SPJ, Lemans JVC, Overweg G, Hekman EEG, Castelein RM, Verkerke GJ, et al. Induction of a representative idiopathic-like scoliosis in a porcine model using a multidirectional dynamic spring-based system. Spine J 2021;21. https://doi.org/10.1016/j.spinee.2021.03.015.

[14] Köhn F, Sharifi AR, Simianer H. Modeling the growth of the Goettingen minipig. J Anim Sci 2007;85:84–92. https://doi.org/10.2527/jas.2006-271.

[15] Dimeglio A. Growth in pediatric orthopaedics. J Pediatr Orthop 2001;21:549–55. https://doi.org/10.1097/01241398-200107000-00026.

[16] Smit TH. The use of a quadruped as an in vivo model for the study of the spine - Biomechanical considerations. Eur Spine J 2002;11:137–44. https://doi.org/10.1007/s005860100346.

[17] Wijdicks SPJ, Lemans JVC, Verkerke GJ, Noordmans HJ, Castelein RM, Kruyt MC. The potential of spring distraction to dynamically correct complex spinal deformities in the growing child. Eur Spine J 2020;1:3. https://doi.org/10.1007/s00586-020-06612-3.

[18] Lemans JVC, Wijdicks SPJ, Castelein RM, Kruyt MC. Spring distraction system for dynamic growth guidance of early onset scoliosis: 2 year prospective follow-up of 24 patients. Spine J 2021;21:671–81. https://doi.org/10.1016/j.spinee.2020.11.007.

[19] Lemans JVC, Tabeling CS, Castelein RM, Kruyt MC. Identifying complications and failure modes of innovative growing rod configurations using the (hybrid) magnetically controlled growing rod and the spring distraction system. Spine Deform 2021;9:1679–89.

[20] Leary S, Underwood W, Anthony R, Cartner S, Greenacre C, Gwaltney-Brant S, et al. AVMA guidelines for Euthanasia of animals:2020 edition. 2020.

[21] Pearcy MJ, Tibrewal SB. Axial rotation and lateral bending in the normal lumbar spine measured by three-dimensional radiography. Spine (Phila Pa 1976) 1984. https://doi.org/10.1097/00007632-198409000-00008.

[22] Willems JM, Jull GA, Ng JKF. An in vivo study of the primary and coupled rotations of the thoracic spine. Clin Biomech 1996. https://doi.org/10.1016/0268-0033(96)00017-4.

[23] Newton PO, Bartley CE, Bastrom TP, Kluck DG, Saito W, Yaszay B. Anterior spinal growth modulation in skeletally immature patients with idiopathic scoliosis: a comparison with posterior spinal fusion at 2 to 5 years postoperatively. J Bone Joint Surg Am 2020;102:769–77. https://doi.org/10.2106/JBJS.19.01176.

[24] Xu L, Sun X, Du C, Zhou Q, Shi B, Zhu Z, et al. Is growth-friendly surgical treatment superior to one-stage posterior spinal fusion in 9- to 11-year-old children with congenital scoliosis? Clin Orthop Relat Res 2020;478:2375–86. https://doi.org/10.1097/CORR.0000000000001377.

[25] Keil LG, Nash AB, Stürmer T, Golightly YM, Lin FC, Stone JD, et al. When is a growth-friendly strategy warranted? A matched comparison of growing rods versus primary posterior spinal fusion in juveniles with early-onset scoliosis. J Pediatr Orthop 2021. https://doi.org/10.1097/BPO.0000000000001926.

[26] Lemans JVC, Kodigudla MK, Kelkar AV, Jayaswal D, Castelein RM, Kruyt MC, et al. Finite element comparison of the spring distraction system and the traditional growing rod for the treatment of early onset scoliosis. Spine (Phila Pa 1976) 2022;47:E456–65. https://doi.org/10.1097/BRS.0000000000004297.

[27] Alanay A, Yucekul A, Abul K, Ergene G, Senay S, Ay B, et al. Thoracoscopic vertebral body tethering for adolescent idiopathic scoliosis: follow-up curve behavior according to sanders skeletal maturity staging. Spine (Phila Pa 1976) 2020;45:E1483–92. https://doi.org/10.1097/BRS.0000000000003643.